Langmuir

ARTICLE

pubs.acs.org/Langmuir

Zwitteration As an Alternative to PEGylation

Zaki G. Estephan, Philip S. Schlenoff, and Joseph B. Schlenoff*

Department of Chemistry and Biochemistry, Florida State University, Tallahassee, Florida 32306, United States

Supporting Information

ABSTRACT: A direct, head-to-head comparison of the efficacy of a zwitterionic versus a poly(ethylene glycol), PEG, coating in preventing protein adsorption to silica and aggregation of silica nanoparticles is presented. The same siloxane coupling chemistry was employed to yield surfaces with similar coverages of both types of ligand. Nanoparticle and planar surfaces were challenged with salt, serum, lysozyme, and serum albumin at 25 and 37 °C. While both types of surface modification are highly effective in preventing protein adsorption and nanoparticle aggregation, the zwitterion provided monolayer-type coverage with minimal thickness, whereas the PEG appeared to yield a more three-dimensional coating. The mechanism for adsorption resistance is thought to be based on preventing ion pairing between protein and surface charges, which releases counterions and water molecules, an entropic driving force enough to overcome a disfavored enthalpy of adsorption.

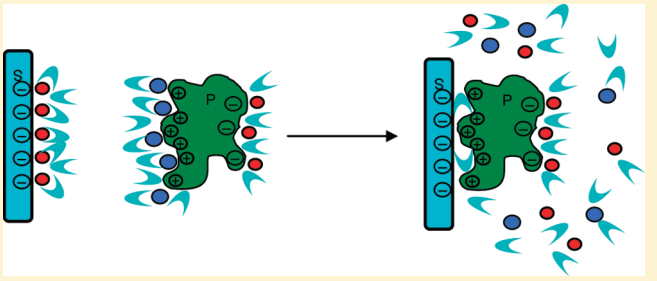

INTRODUCTION

Exposure of surfaces to proteins in solution triggers a set of adsorption steps that controls subsequent surface interactions.[1−3] For biosensors, nonspecific adsorption degrades the performance of the device or leads to false positives in some cases.[3−5] In nanomedicine, the adsorption of plasma proteins onto the nanovehicle dictates its residence time in blood and its ultimate destination.[1,2] Thus, passivating surfaces against nonspecific interactions has been an active field for the last few decades. The term "PEGylation" refers to the widespread practice of attaching oligomeric or polymeric ethylene glycol units (polyethylene glycol) to surfaces or molecules for the purpose of enhancing biocompatibility and biodistribution. For suppression of protein adsorption to surfaces, PEG has been the standard against which new materials are judged.[6−8] However, the temperature dependence of PEG[9] and its autooxidation catalyzed by transition metals present in most biological systems[10] have directed the search toward new classes of biocompatible surfaces, wherein zwitterions are promising candidates.[11−15]

Various models have been proposed to explain the ability of PEG to repel proteins. Jeon et al. related the resistive properties to steric repulsion with an elastic and an osmotic component.[16,17] In their model, repulsion was attributed to the entropically disfavored compression of polymer chains and the presence of a strong hydration layer that prevents close encounter with proteins. This model was challenged by Harder et al. and Wang et al., who argued that it does not explain the resistive properties of small oligomeric chains.[18,19] Instead, the conformation of the oligomeric ethylene glycol on the surface, helical vs "all-trans", which affects the interfacial water layer, was proposed to influence protein adsorption. Water molecules were suggested to be loosely bound to the all-trans form and were thus easily replaced with the approaching protein molecule in contrast to the helical conformation where a strong hydration layer prevents close contact.[18,19] In discussing the role of packing density, Li et al. argued that hydration and conformational flexibility of chains are important to resistive properties.[20] Regardless of the model, protein adsorption studies on PEG-grafted surfaces have been contradicting in certain cases, either with respect to the effect of molecular structure on adsorption or in terms of its temperature dependence.[9,20−22] While these theories capture, within constraints, the repulsive origin of PEG, they do not provide an explanation for other known protein-repellent surfaces. In an alternative approach, Kane et al., after screening a number of protein-resistive molecules, concluded that osmolytes are preferentially excluded from protein surfaces and thus hypothesized that kosmotropes form the basis of protein-repellent surfaces.[13] Although such a classification is consistent, it still does not give a molecular description of the mechanism of protein resistance. Some characteristics are widely agreed upon, however, for all protein-repellent surfaces, such as electrical neutrality, hydrophilicity, and the ability to accept, but not donate, a hydrogen bond.[12]

Adsorption can only occur if the total free energy is negative ($\Delta G_{ads} = \Delta H_{ads} - T\Delta S_{ads} < 0$). Endothermic heats of adsorption, often reported, lead to the conclusion that the driving force for adsorption must be entropic in nature, attributed to the release of water molecules (hydrophobic dehydration) or counterions or alterations in the structure of the protein molecule (conformational entropy).[23−25] For example, the adsorption of

Received: January 18, 2011
Revised: April 11, 2011
Published: May 02, 2011

BSA, a "soft" protein, on negatively charged silica is thought to be governed by an entropically favored conformational change that offsets the endothermicity of interactions.[26,27] For hydrophobic surfaces, such as polystyrene, hydrophobic dehydration is responsible for the adsorption.[28] On the other hand, hydrophobic dehydration cannot be the answer when hydrophilic surfaces are involved nor can the minute conformational changes in "hard" proteins rationalize the interaction when the endothermic penalty is too high.

Inspired by the zwitterionic character of most cell membranes, we recently reported on the stabilization of gold and silica nanoparticles using small zwitterionic disulfide and siloxane molecules, respectively.[29,30] The nanoparticles showed excellent stability in solutions of high salt concentration, classical colloid destabilizers, and media representing the chemical complexity of an in vivo environment. These results led us to question, in the present work, whether there are any significant differences or advantages to the use of short-chain PEGs versus zwitterions in the stabilization of surfaces, in particular nanoparticles, and to propose a mechanism for protein resistance that would be consistent with both types of surface modification. The aggregation of nanoparticles was tested in solutions of different salt concentrations or in protein solutions. The adsorption of two model proteins, BSA, a large protein with the same net charge sign as that of the native silica, and lysozyme, a small "sticky" positive protein, was followed using ellipsometry on planar surfaces. Because the repulsive properties of PEG have been questioned above 35 °C, studies were carried out at 25 and 37 °C.

EXPERIMENTAL SECTION

Materials. Ludox TM-40 colloidal silica (surface area reported by manufacturer, 140 $m^2\ g^{-1}$) 40 wt % suspension in water was used as received from Sigma-Aldrich. Methyl-terminated PEG siloxane, 2-[methoxy(polyethyleneoxy)propyl]trimethoxy silane (tech-90, 6−9 ethylene oxide repeat units as reported by the manufacturer, 460−590 g mol^{-1}), and (*N*,*N*-dimethyl-3-aminopropyl)trimethoxy silane were purchased from Gelest, stored under Ar, and used as received. Fetal bovine serum (VWR) and lysozyme (from chicken egg white, protein ≥ 90%, Sigma Aldrich) were stored at −20 °C. Bovine albumin, fraction V (BSA, Sigma-Aldrich, 99%), was stored at 4 °C. Sodium phosphate monobasic (ACS grade), sodium phosphate (ACS grade), and NaCl (ACS grade) were from Fisher Scientific. Propane sultone was obtained from TCI America. Spectra/Pro dialysis tubing (MWCO 3 500) was from VWR.

Experimental Methods. The zwitterion siloxane 3-(dimethyl-(3-(trimethoxysilyl)propyl)ammonio)propane-1-sulfonate (sulfobetaine siloxane or SBS, 329.5 g mol^{-1}) was synthesized as described previously[30] using (*N*,*N*-dimethyl-3-aminopropyl)trimethoxy silane and propane sultone. The structures of SBS and PEG siloxane are shown in the Supporting Information.

^{1}H NMR was used to calculate the average number of ethylene glycol repeat units in PEG siloxane. In this case the signal from the terminal methoxy ether ^{1}H at δ 3.37 ppm was fixed to three, and the total signal from the ethylene ether ^{1}H at δ 3.69 ppm was divided by the theoretical four ^{1}H of the ethylene glycol (EG) unit. The experimental average number of repeat units was 9.

The hydrolysis rate of the two siloxanes in water was followed with ^{1}H NMR. Measurements were performed at rt in D_2O with a Bruker Ultrashield 600 MHz NMR. A 35 mg amount of the siloxane was dissolved in 600 μL of D_2O at rt, and the decrease in the peak area for the methoxy signal at δ 3.6 ppm normalized to the theoretical 9 methoxy ^{1}H was monitored versus time.

Nanoparticle Modification. Different amounts of methoxy PEG siloxane or SBS were added to 10 wt % final concentration Ludox silica (17 nm hydrodynamic radius) at rt. After 3 h, the reaction mixture was heated at 80 °C for an additional 3 h. The solution was then allowed to cool to rt and then dialyzed against 18 MΩ H_2O for 12 h. The final solution wt % was calculated by drying 1 mL of the solution at 25 °C under vacuum.

The amount of siloxane bonded to the silica surface was determined from thermogravimetric analysis, TGA (SDT Q600, TA Instruments). A few milligrams of the dried nanoparticles were placed in a platinum cup inside an oven under N_2 at a flow rate of 100 mL min^{-1}. The temperature of the oven was ramped to 105 °C and held for 20 min to ensure desorption of adsorbed water, after which the temperature was ramped to 800 °C at a rate of 10 °C min^{-1}. Bare silica nanoparticles and hydrolyzed siloxanes were run in the same way to aid in translating the TGA results to calculated surface coverage. The siloxanes were first hydrolyzed in water and then freeze dried in order to mimic the reaction conditions.

The stability of the modified silica nanoparticles was assessed with turbidimetry by monitoring the increase in absorbance (indicative of aggregation) at 500 nm using a Varian Cary 100 UV−vis double beam spectrophotometer. Nanoparticles were dispersed in the buffer at a final concentration of 1 wt % and the absorbance recorded following addition of salt (0.5 or 3.0 M NaCl in phosphate buffer) or protein (10% v/v FBS in PBS). Experiments were performed at 25 or 37 °C to assess the effect of temperature on the properties of the modified nanoparticles.

Dynamic light scattering (DLS) was used to measure the size of silica nanoparticles. Approximately 100 μL of dialyzed nanoparticles was dispersed in 10 mL of 10 mM PBS (140 mM NaCl, pH 7.4) pumped through the flow cell at a flow rate of 10 mL h^{-1}. The adsorption of protein onto modified and bare silica nanoparticles was assessed by monitoring the increase in particle size in the presence of BSA ($10 \times 4 \times 4\ nm^3$)[31] and lysozyme (approximate dimensions $3.0 \times 3.0 \times 4.5\ nm^3$)[32] in PBS. The concentration of protein in the buffer was fixed at 0.1 wt %, and that of nanoparticles was 0.5 and 0.1 wt % for BSA and lysozyme, respectively. Samples were prepared in a microcuvette and introduced into a temperature-controlled cell holder. Readings were collected as a function of incubation time at 25 or 37 °C. DLS measurements were performed with a Wyatt QELS instrument collecting at 108° to the incident 690 nm laser beam in a Wyatt DAWN EOS instrument with a 20 s collection interval and analysis with ASTRA 5.3.4 software.

Planar Surfaces. Adsorption of protein onto planar surfaces was also measured to illustrate the effect of the substrate geometry on the behavior of the grafted surface toward protein adsorption. Silicon wafers were cleaned with RCA solution (28% NH_4OH:30% H_2O_2:H_2O 1:1:5) for 10 min followed by extensive rinsing with 18 MΩ H_2O. The wafer was then treated with cold piranha (concentrated H_2SO_4:30% H_2O_2 7:3. *Warning*: do not store in closed containers) for 10 min followed by rinsing with fresh water. This resulted in a hydrophilic oxide layer with a near-zero contact angle and a thickness of ∼20 Å. The silicon wafers were then placed in 0.1 M aqueous solution of methoxy PEG or SBS at 80 °C for 15 h. After rinsing the wafer with water, contact angle and thickness measurements were taken.

The adsorption of proteins, 0.1 wt % BSA or lysozyme, from PBS buffer was studied on untreated and siloxane-treated silicon at 25 and 37 °C. Wafers were immersed in a temperature-controlled cell and then removed at different time intervals. 1, 2, 4, 8, 16, 32, and 64 min, followed by quick rinsing steps in PBS and water, respectively, and gentle drying with a stream of N_2. The thickness after dipping was subtracted from that measured after PEGylation or zwitteration. An increase of thickness was taken as an indication of adsorption. Contact angles for the 30 min immersion time samples were also measured. Results are the average of 3 trials. Contact angles were recorded on a KSV Cam 200 instrument by dispensing 10 μL of water on the silicon wafer. Thickness was measured

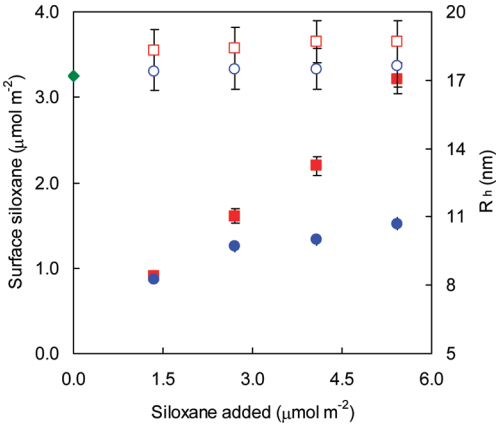

Figure 1. Surface coverage of silica nanoparticles from TGA (solid symbols) and hydrodynamic radii from DLS (open symbols) as a function of the amount of siloxane added to solution: zwitterion siloxane (blue solid circles, blue open circles) and PEG siloxane (red solid squares, red open squares). The hydrodynamic radius of the untreated SiO_2 is also shown (green diamonds).

with ellipsometry (Gaertner Scientific) with a 632.8 nm He−Ne laser fixed at a 70° angle incident to the sample.

RESULTS AND DISCUSSION

Addition of siloxane to silica nanoparticles was validated by DLS and TGA measurements. No major change in hydrodynamic radius was observed with either silylation agent; however, the PEGylated nanoparticles were consistently larger than the zwitterated and bare silica nanoparticles by about 1 nm (Figure 1). The amount of surface siloxane per square meter of silica as a function of solution siloxane concentration was calculated from TGA assuming complete hydrolysis of the methoxy groups and that each siloxane molecule anchors to one surface silanol and two neighboring siloxanes resulting in surface polymerization.[33] As shown in Figure 1, increasing SBS solution concentration beyond that theoretically needed for a coverage of ca. 3 μmol m^{-2} does not result in an additional increase in surface concentration, which saturates at around 1.5 ± 0.2 μmol m^{-2}, consistent with our previous report, indicating the absence of 3D network polymerization.[30] In contrast, PEG surface concentration increases with the amount of siloxane added with no apparent surface saturation. This can be related to formation of a polymeric network where condensation occurs in solution or with surface siloxane instead of surface silanol consistent with the large body of literature on the modification of silica surfaces.[34−36] Monitoring the hydrolysis rate of the two siloxanes in water revealed that the observed higher PEG surface concentration is not the result of faster hydrolysis (Figure S1, Supporting Information). In fact, the half-life of SBS in water was short (ca. 1 h) in comparison with that of PEG siloxane (ca. 12 h), suggesting that some of the PEG might have deposited on the surface with partial hydrolysis of its methoxy groups. It thus seems that silylation using SBS is more controlled, yielding monolayer coverage, and condensing only with the surface. For subsequent studies we chose the zwitterated silica nanoparticles with SBS surface coverage of 1.25 μmol m^{-2} (reported hereafter as 1.25 μmol Zwi m^{-2}) and the PEGylated silica nanoparticles with PEG surface coverage of 1.61 μmol m^{-2} (reported as 1.61 μmol PEG m^{-2}). These samples were a result of addition of the same amount of siloxane in solution (Figure 1) that would yield what is believed to be about monolayer coverage for both.

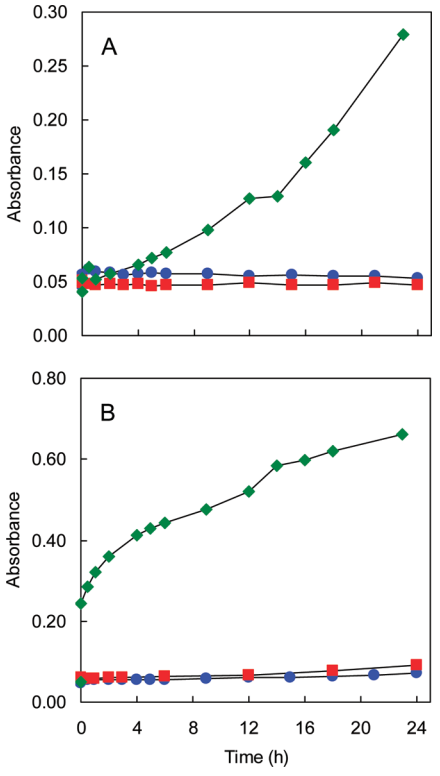

Figure 2. Turbidimetry at 500 nm and 37 °C showing the effect of (A) 0.5 M NaCl in 10 mM phosphate buffer (pH 7.4) and (B) 10% v/v FBS in 10 mM PBS (140 mM NaCl, pH 7.4) on the behavior of untreated SiO_2 (green diamonds), 1.61 μmol PEG m^{-2} SiO_2 (red squares), and 1.25 μmol Zwi m^{-2} SiO_2 (blue circles). Nanoparticle concentration is 1 wt %.

The stabilities of PEGylated versus zwitterated nanoparticles were compared head-to-head at two temperatures in different salt concentrations and in 10% v/v FBS solution by turbidimetry at 500 nm. Bare silica nanoparticles showed expected DLVO theory behavior in salt solutions where aggregation was observed at higher concentrations of salt (Figures 2A and 3).[37] Aggregation of the bare silica nanoparticles was also rapidly induced by FBS due to adsorption of proteins from the serum medium (Figure 2B). In contrast to the bare silica surface, both zwitterated and PEGylated nanoparticles showed no sign of aggregation over 24 h, regardless of the temperature when studied in FBS or in 0.5 M NaCl (Figures 2 and S2, Supporting Information). However, increasing the salt concentration to 3 M and raising the temperature to 37 °C (Figure 3B) results in rapid aggregation of the PEGylated nanoparticles, in agreement with the behavior of PEG in aqueous salt solutions.[38] This is attributed to loss of the hydration layer at elevated temperature, resulting in exposure of its hydrophobic character and causing its precipitation. This behavior is not observed for zwitterated silica nanoparticles, consistent with the increased solubility of zwitterions at higher ionic strength.[39]

The in situ adsorption of proteins from a single-component medium was followed by DLS. Serum albumin, the major component in blood serum, was incubated with nanoparticles at 37 °C. BSA has been reported to adsorb nonspecifically on silica surfaces.[28,40,41] This adsorption is said to increase circulation

dx.doi.org/10.1021/la200227b |*Langmuir* 2011, 27, 6794–6800

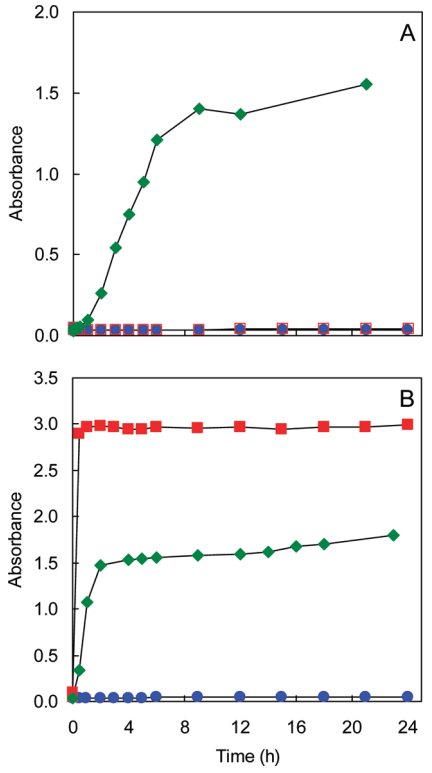

Figure 3. Turbidimetry vs time at 500 nm showing the effect of temperature on the aggregation of untreated SiO_2 (green diamonds), 1.61 μmol PEG m^{-2} SiO_2 (red squares), and 1.25 μmol Zwi m^{-2} SiO_2 (blue circles) in 3 M NaCl buffered in 10 mM phosphate buffer at pH 7.4. Experiment was performed at (A) 25 and (B) 37 °C. Nanoparticle concentration is 1 wt %.

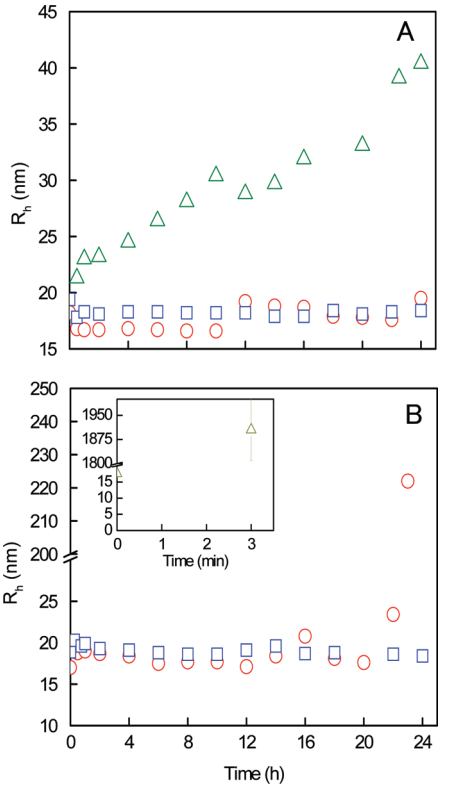

Figure 4. DLS study of untreated SiO_2 (green triangles), 1.61 μmol PEG m^{-2} SiO_2 (blue squares), and 1.25 μmol Zwi m^{-2} SiO_2 (red circles) in the presence of negatively charged BSA and positively charged lysozyme in 10 mM PBS (140 mM NaCl, pH 7.4) at 37 °C: (A) 0.5 wt % nanoparticle concentration and 0.1 wt % BSA and (B) 0.1 wt % nanoparticles and 0.1 wt % lysozyme. Error bars are of the same size as the symbols.

time in blood.[2] Figure 4A shows the hydrodynamic radius of the untreated silica nanoparticles steadily increased to ca. 40 nm after 24 h, whereas the size of the coated silica remained constant. The DLS showed a small instantaneous drop of about 2 nm in the observed R_h due to the contribution of the protein to the overall scattering. Although scattering intensity is a strong, nonlinear function of size, DLS is unable to resolve the BSA/silica bimodal particle size distribution here with the result that the correlation function is interpreted as a slightly smaller particle. A slight increase of radius in the zwitterated silica, seen after about 10 h, may reflect adsorption of some BSA after this time. Prior work on the adsorption of BSA to bare silica NPs has shown that about one-half a monolayer accumulates irreversibly.[41] The R_h for bare NPs drifts up to values considerably more than a monolayer, suggesting multilayer adsorption and/or partial aggregation for this system.

Single-component protein systems are not good predictors of protein coverage in the blood environment. It has been shown that the composition of the "corona" of proteins attaching to nanoparticles does not at all match the plasma composition.[42] For example, despite the overwhelming prevalence of serum albumin, its surface composition on silica NPs immersed in 10% plasma is only 2% of the total protein corona, due to weak interactions, relative to other plasma proteins, with silica.[42] Thus, lysozyme, a protein known to adsorb strongly to silica, was employed here as an example of a strong challenge to the surface passivation chemistry. Silica, negatively charged at physiological pH, interacts electrostatically with the positively charged lysozyme.

As expected, addition of lysozyme to bare silica nanoparticles resulted in a rapid increase in measured hydrodynamic radius within minutes, supporting turbidimetry measurements and in agreement with previously reported results (insets in Figures 4B and S3, Supporting Information).[30,43] Functionalization of the silica surface with PEG or zwitterion enhanced the particles' ability to resist protein adsorption. This behavior was more prolonged with the PEGylated nanoparticles where adsorption was not observed within the experimental time frame, whereas zwitterated nanoparticles increased in size about 20 h after lysozyme addition (Figures 4B and S3, Supporting Information). It should be noted however that although the hydrodynamic radius for the zwitterated nanoparticles increased after 20 h, their corresponding number distribution revealed that the majority of the particles were still in the 17 nm range (Figure S4, Supporting Information). The corresponding increase in observed size is due to a small fraction of aggregates resulting in higher scattering due to the dependence of the intensity of scattered light on the sixth power of size, thus skewing the reported hydrodynamic radius. For drug delivery, prolonged circulation of the vehicle in the blood is desired in order for it to reach its desired target. However, an efficient clearing mechanism is also needed in order to avoid any side effects that might arise due to the presence of the nanovehicle.[44] A delicate balance between the above factors is hence required to ensure safe application of nanomaterials. The increase in size after 20 h may therefore be beneficial for the

dx.doi.org/10.1021/la200227b |*Langmuir* 2011, 27, 6794–6800

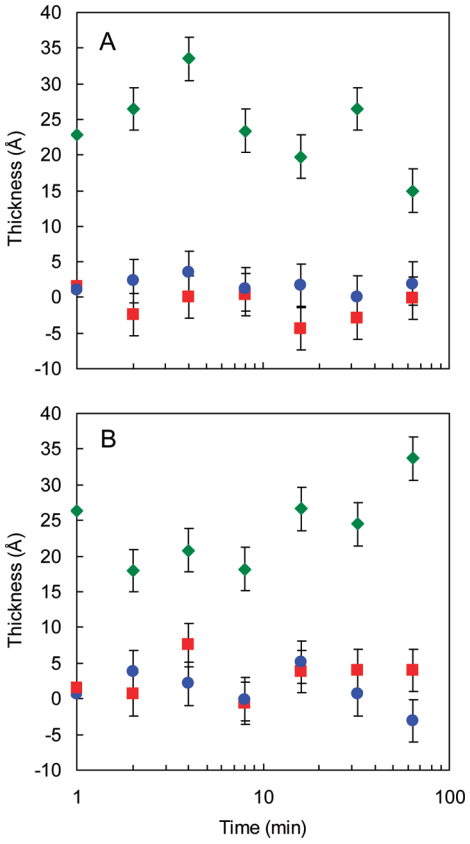

Figure 5. Adsorption of BSA (A) and lysozyme (B) from 0.1 wt % solution in 10 mM PBS (140 mM NaCl, pH 7.4) at 37 °C onto untreated (green diamonds), PEGylated (red squares), and zwitterated (blue circles) silicon wafer.

clearance of the particles from the system after desired targeting has been achieved. Such delayed destabilization is a fortuitous example of "programmed" loss of biocompatibility or circulation.

Finally, we compared the two siloxanes on planar substrates in a more classical protein adsorption experiment. Silicon wafers treated with either SBS or PEG siloxane were immersed in 0.1 wt % BSA or lysozyme at 25 or 37 °C for different time intervals. As a control, a clean unmodified wafer was used. At both temperatures studied, the untreated silicon wafer showed a rapid increase in thickness of around 20 Å after 1 min of dipping and either continued to gradually increase in thickness or remained constant depending on the temperature. PEGylated and zwitterated surfaces on the other hand showed little to no increase in thickness (Figures 5 and S5, Supporting Information), indicating no adsorption or submonolayer coverage. These are in agreement with previous adsorption studies on similar surfaces where less than 3% of monolayer coverage has been reported.[13,45] The contact angle before and 30 min after dipping was also measured to detect any changes. The untreated silicon wafer showed an increase from 0° to 35 ± 5° in BSA and 45 ± 5° in lysozyme, whereas that of PEGylated and zwitterated surfaces remained unchanged (<5° for zwitterated and 40 ± 3° for PEGylated). Contact angle thus correlates well with the results obtained from ellipsometry, confirming the absence of adsorption on PEGylated or zwitterated surfaces.

Insights into the Mechanism of Protein Adsorption. Adsorption occurs if the total free energy of the system is reduced.

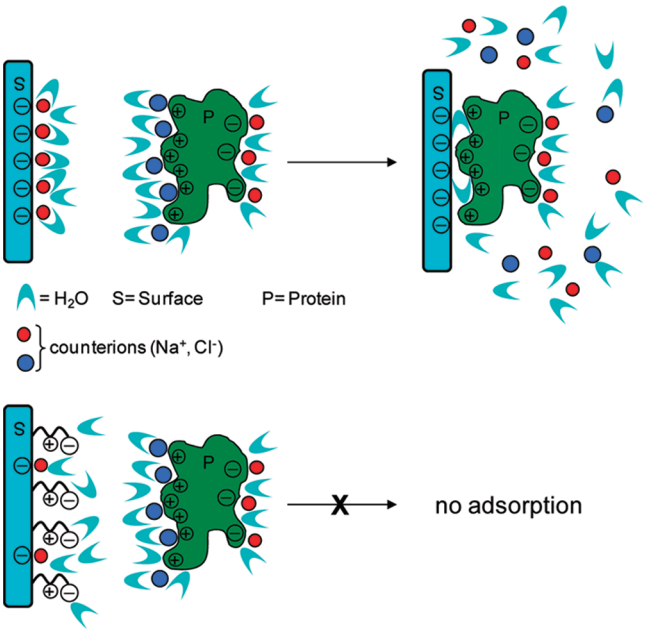

Figure 6. Cartoon for the ion-coupled adsorption mechanism of a protein with a net positive charge onto a negatively charged hydrophilic substrate. (Top) Adsorption of protein is facilitated by the release of counterions and formation of ion pairs between the sorbent and the adsorbate. (Bottom) Neutral surface (zwitterion or PEG) has no surface ions associated with it. The binding of protein to the surface will not result in a net increase in entropy due to counterion release, and thus, adsorption is not preferred. Note that some of the charge is still associated with the original surface but is inaccessible due to a steric barrier.

The enthalpic contribution to the adsorption of lysozyme or BSA onto silica has been reported to be positive, indicating that the process is driven by entropy.[26,27,46] Hydrophobic dehydration of the sort reported for polystyrene cannot be adopted for the hydrophilic silica surface, and thus, other factors should come into play to account for adsorption. BSA is a "soft" protein, and its adsorption is thus facilitated, to a certain extent, by conformational changes.[47] The extent of conformational changes in lysozyme, a "hard" protein, is reported to be low,[32,48] and the entropy gain due to this process cannot be enough to drive the adsorption process. The adsorption is thus mainly explained in terms of electrostatic attraction between the oppositely charged surfaces, a process that should be *exothermic*.

In order to explain the highly effective resistance to protein adsorption for both PEG- and zwitterion-modified surfaces we adapt some of the ideas behind the complexation of proteins with charged polymers, where the driving force for association has been proposed by some to be release of counterions.[25,49−51] The negative surface charge of the silica surface is counterbalanced by cations (e.g., Na^+). Proteins bear numerous charges balanced by the appropriate counterion. While the entire protein has a net charge, patches of positive or negative charges exist and are thought to play a role in the adsorption of the protein to a surface with the same net charge as the protein.[52,53] As shown in Figure 6, the adsorption of a positive protein, or positive patch of a net negative protein to silica, results in formation of an ion pair and release of counterions. Each ion pair formed releases two counterions. As we described recently,[54] ion pair formation as the driving force for an athermal or net endothermic complexation between polymers of opposite charge also involves release of water molecules. Roughly

dx.doi.org/10.1021/la200227b |*Langmuir* 2011, 27, 6794–6800

speaking, the net entropy gain would be kT for each ion or water molecule released. For a neutral surface, such as a zwitterion or PEG moiety, the surface charge is internally balanced (zwitterion) or neutral (PEG) and formation of an ion pair with the adsorbate is unlikely; no ions are available for release from the surface.

Kane et al. reported that zwitterionic surfaces adsorb little protein at low salt concentration but are completely repellent at high salt concentration.[13] They also reported that zwitterionic surfaces made of mixed SAMs were resistive at all ionic strengths studied. For SAMs carrying the zwitterionic character on the same molecule, a slight variation of charge ratio due to impurities will lead to charge accumulation on the surface and consequent adsorption at low ionic strength, as supported by Chen et al., who observed the effect of charge imbalance of phosphorylcholine SAMs on the adsorption behavior.[55] A similar rationale applies for PEG surfaces. Pasche et al., who studied the interfacial forces between PEG-*g*-PLL adlayers on a Nb_2O_5 surface and proteins using colloidal-probe AFM,[56,57] found that at low surface density the surface charges "shine through" the PEG layer and strongly repel the probe. Only when the PEG surface density and its thickness were large enough to completely encompass the electrostatic double layer did the steric effect come into play.

We believe the major driving force for the resistance of protein on PEGylated surfaces is mainly due to the lack of ion release and not to entropy from chain compression or restricted mobility. A central tenet of this rationalization for protein resistance is that adsorption can be divided into *ion-coupled* and *ion-decoupled* mechanisms. The ion-coupled mechanism, described above, is essentially an ion-exchange process dominated by entropic release of ions and attendant water molecules, whereas an ion-decoupled mechanism does not involve rearranging counterions and may rely on dipole−dipole, hydrogen bonding, van der Waals, or other interactions. The role of "hydrophobicity" is complex and should be separated into an ion-coupled component, where water molecules are lost as a result of ion pair formation, and an ion-decoupled component, which might involve water restructuring or a decrease in surface energy as a result of a hydrophobic portion of a protein adsorbing to a hydrophobic surface. The latter interaction should be exothermic.

There is a "steric" component to ion-coupled adsorption. Although we were able to completely suppress the surface charge of zwitterated silica (SiZwi) nanoparticles,[30] we observed effective resistance to protein adsorption for SiZwi with a significant negative surface charge.[30] We believe that although these particles are charged, access to the surface site, and therefore release of the surface counterion, is blocked for steric reasons. The diagram in Figure 6 illustrates this concept. In other words, the "steric" role of adsorbed neutral barriers is to prevent access to and release of surface-bound counterions by ion pair formation. The final role of neutral, hydrophilic protein-resistant coatings is to minimize ion-decoupled hydrophobic interactions. PEG fails to prevent aggregation at 37 °C in salt (Figure 3B), probably because the chains are dehydrated due to the higher temperature (PEG exhibits a LCST) and the dehydrating effect (via osmotic pressure) of the 3 M NaCl.

Some rough estimates of ion-coupled driving forces available for protein adsorption may be made, starting with the condition that $T\Delta S$ must be larger than ΔH for adsorption. Focusing on one adsorption site; each ion pair formation results in an entropy gain of kT for each ion or water molecule released. While the number of ions released is 2 for Na^+ and Cl^- as participating counterions, the number of water molecules released, z_{H_2O}, is less clear. In the association of sulfonate and amino or quaternary ammonium sites on polyelectrolytes we found z_{H_2O} to be about 4.[54] The total energy available per m^2 is

$$T\Delta S = \left(2 + z_{H_2O}\right)kT\Psi \quad (1)$$

where Ψ is the charge density of the surface (m^{-2}).

Equation 1 can be compared to data on BSA adsorption. Typical coverages for BSA adsorbed on silica at 25 °C and pH 7 are in the range of 0.8−1.5 mg m^{-2} depending on the buffer and ionic strength.[28,40,58] Assuming 1 mg m^{-2} and an enthalpy of +47 J g^{-1} protein as reported by Kulikova et al.,[27] the enthalpic contribution per m^2 is +47 mJ m^{-2}. If we assume 2 ions and 4 water molecules are released on adsorption to a site, the entropic gain is 6 kT per site or 119 mJ m^{-2} assuming a surface charge density for silica of 8 μmol m^{-2} at pH 7 and 25 °C.[59] Thus, the adsorption of a positive patch of BSA onto the negatively charged silica surface is favorable with an adsorption free energy of −72 mJ m^{-2}. If we assume that the zwitterion or PEG gives monolayer coverage (a better assumption for the zwitterion siloxane than for the PEG siloxane, see Figure 1) and we define critical coverage Γ_c as the fraction of a full monolayer needed to prevent adsorption via an ion-coupled mechanism, then

$$\left(2 + z_{H_2O}\right)kT\Psi(1 - \Gamma_c) = \Delta H_{ads} \quad (2)$$

Equation 2 assumes no contribution from solution ions to the overall energy balance. While the ionic strength of the medium is usually maintained at physiological (e.g., 0.15 M NaCl), additional salt works to decrease the adsorption driving force (or to lower the amount of siloxane surface coverage required) via the ion-coupled mechanism. This effect has been observed.[50]

CONCLUSION

A comparison between PEGylated and zwitterated surfaces was performed at 25 and 37 °C in different salt concentrations using two model proteins. At planar surfaces no evidence was seen for protein adsorption at either surface. For nanoparticles, PEGylation stabilizes the particles in salt solutions as long as the temperature is below a lower critical solution temperature. In contrast, zwitterated surface are stable regardless of the temperature and salt concentration. Both zwitterated and PEGylated nanoparticles were also found to resist aggregation in the presence of serum. DLS showed that when exposed to lysozyme zwitterated nanoparticles are stable for ∼20 h, after which the hydrodynamic radius starts to increase, whereas PEGylated nanoparticles resist adsorption for longer periods. As with oligomeric PEGs, zwitterions are short molecules which cannot suffer the reduction of degrees of freedom on protein adsorption ("entropic penalty"). The mechanism of protein resistivity is believed to be due to the absence of counterion release, which would otherwise result in an entropy gain. If the enthalpy of adsorption is positive, only a fraction of the charge on the surface needs to be removed to decrease the entropic gain enough to prevent adsorption.

ASSOCIATED CONTENT

Supporting Information. Hydrolysis rate of siloxanes, structure of siloxanes, turbidimetry results in 0.5 M NaCl and in 10% v/v FBS at 25 °C, DLS results in the presence of lysozyme at 25 °C, hydrodynamic radii distribution, and ellipsometry results

for adsorption on planar surfaces at 25 °C. This material is available free of charge via the Internet at http://pubs.acs.org.

AUTHOR INFORMATION

Corresponding Author
*E-mail: schlen@chem.fsu.edu.

ACKNOWLEDGMENT

This work was supported by Florida State University. We thank Dr. Andreas Reisch for his help with ^{1}H NMR measurements.

REFERENCES

(1) Owens, D. E.; Peppas, N. A. *Int. J. Pharm.* **2006**, *307*, 93–102.
(2) Aggarwal, P.; Hall, J. B.; McLeland, C. B.; Dobrovolskaia, M. A.; McNeil, S. E. *Adv. Drug Delivery Rev.* **2009**, *61*, 428–437.
(3) Park, S.; Hamad-Schifferli, K. *Curr. Opin. Chem. Biol.* **2010**, *14*, 616–622.
(4) Jass, J.; LappinScott, H. M. *Chem. Ind., London* **1997**, 682–685.
(5) Schneider, B. H.; Dickinson, E. L.; Vach, M. D.; Hoijer, J. V.; Howard, L. V. *Biosens. Bioelectron.* **2000**, *15*, 13–22.
(6) Leckband, D.; Sheth, S.; Halperin, A. *J. Biomater. Sci., Polym. Ed.* **1999**, *10*, 1125–1147.
(7) Thierry, B.; Zimmer, L.; McNiven, S.; Finnie, K.; Barbé, C.; Griessert, H. J. *Langmuir* **2008**, *24*, 8143–8150.
(8) Zalipsky, S.; Harris, J. M. *ACS Symp. Ser.* **1997**, *680*, 1–13.
(9) Efremova, N. V.; Sheth, S. R.; Leckband, D. E. *Langmuir* **2001**, *17*, 7628–7636.
(10) Luk, Y. Y.; Kato, M.; Mrksich, M. *Langmuir.* **2000**, *16*, 9604–9608.
(11) Ostuni, E.; Chapman, R. G.; Liang, M. N.; Meluleni, G.; Pier, G.; Ingber, D. E.; Whitesides, G. M. *Langmuir* **2001**, *17*, 6336–6343.
(12) Holmlin, R. E.; Chen, X. X.; Chapman, R. G.; Takayama, S.; Whitesides, G. M. *Langmuir* **2001**, *17*, 2841–2850.
(13) Kane, R. S.; Deschatelets, P.; Whitesides, G. M. *Langmuir* **2003**, *19*, 2388–2391.
(14) Breus, V. V.; Heyes, C. D.; Tron, K.; Nienhaus, G. U. *ACS Nano* **2009**, *3*, 2573–2580.
(15) Muro, E.; Pons, T.; Lequeux, N.; Fragola, A.; Sanson, N.; Lenkei, Z.; Dubertret, B. *J. Am. Chem. Soc.* **2010**, *132*, 4556–4557.
(16) Jeon, S. I.; Lee, J. H.; Andrade, J. D.; Degennes, P. G. *J. Colloid Interface Sci.* **1991**, *142*, 149–158.
(17) Jeon, S. I.; Andrade, J. D. *J. Colloid Interface Sci.* **1991**, *142*, 159–166.
(18) Wang, R. L. C.; Kreuzer, H. J.; Grunze, M. *J. Phys. Chem. B* **1997**, *101*, 9767–9773.
(19) Harder, P.; Grunze, M.; Dahint, R.; Whitesides, G. M.; Laibinis, P. E. *J. Phys. Chem. B* **1998**, *102*, 426–436.
(20) Li, L. Y.; Chen, S. F.; Zheng, J.; Ratner, B. D.; Jiang, S. Y. *J. Phys. Chem. B* **2005**, *109*, 2934–2941.
(21) Schwendel, D.; Dahint, R.; Herrwerth, S.; Schloerholz, M.; Eck, W.; Grunze, M. *Langmuir* **2001**, *17*, 5717–5720.
(22) Norde, W.; Gage, D. *Langmuir* **2004**, *20*, 4162–4167.
(23) Norde, W. *Adv. Colloid Interface Sci.* **1986**, *25*, 267–340.
(24) Norde, W. *Pure Appl. Chem.* **1994**, *66*, 491–496.
(25) Record, M. T.; Anderson, C. F.; Lohman, T. M. *Q. Rev. Biophys.* **1978**, *11*, 103–178.
(26) Norde, W.; Macritchie, F.; Nowicka, G.; Lyklema, J. *J. Colloid Interface Sci.* **1986**, *112*, 447–456.
(27) Kulikova, G. A.; Ryabinina, I. V.; Guseynov, S. S.; Parfenyuk, E. V. *Thermochim. Acta* **2010**, *503*, 65–69.
(28) Norde, W. *NATO Adv. Sci. I, Ser. E: Appl. Phys.* **1997**, *335*, 541–555.
(29) Rouhana, L. L.; Jaber, J. A.; Schlenoff, J. B. *Langmuir* **2007**, *23*, 12799–12801.
(30) Estephan, Z. G.; Jaber, J. A.; Schlenoff, J. B. *Langmuir* **2010**, *26*, 16884–16889.
(31) Wright, A. K.; Thompson, M. R. *Biophys. J.* **1975**, *15*, 137–141.
(32) Arai, T.; Norde, W. *Colloids Surf.* **1990**, *51*, 1–15.
(33) Sindorf, D. W.; Maciel, G. E. *J. Am. Chem. Soc.* **1983**, *105*, 3767–3776.
(34) Blum, F. D.; Meesiri, W.; Kang, H. J.; Gambogi, J. E. *J. Adhes. Sci. Technol.* **1991**, *5*, 479–496.
(35) Van Der Voort, P.; Vansant, E. F. *Pol. J. Chem.* **1997**, *71*, 550–567.
(36) Fadeev, A. Y.; McCarthy, T. J. *Langmuir* **2000**, *16*, 7268–7274.
(37) In *Colloidal Silica: Fundamentals and Applications*; Bergna, H. E., Roberts, W. O., Eds.; CRC Press: Boca Raton, 2006.
(38) Ataman, M. *Colloid Polym. Sci.* **1987**, *265*, 19–25.
(39) Lowe, A. B.; McCormick, C. L. *Chem. Rev.* **2002**, *102*, 4177–4189.
(40) Larsericsdotter, H.; Oscarsson, S.; Buijs, J. *J. Colloid Interface Sci.* **2005**, *289*, 26–35.
(41) Turci, F.; Ghibaudi, E.; Colonna, M.; Boscolo, B.; Fenoglio, I.; Fubini, B. *Langmuir* **2010**, *26*, 8336–8346.
(42) Monopoli, M. P.; Walczyk, D.; Campbell, A.; Elia, G.; Lynch, I.; Bombelli, F. B.; Dawson, K. A. *J. Am. Chem. Soc.* **2011**, *133*, 2525–2534.
(43) Jia, G. W.; Cao, Z. Q.; Xue, H.; Xu, Y. S.; Jiang, S. Y. *Langmuir* **2009**, *25*, 3196–3199.
(44) Oberdorster, G. Biokinetics and effects of nanoparticles. In *NATO Science Peace Secur*; Simeonova, P. P., Opopol, N., Luster, M. I., Eds.; Springer: Dordrecht, 2007; pp 15−51.
(45) Zhang, Z.; Zhang, M.; Chen, S. F.; Horbetta, T. A.; Ratner, B. D.; Jiang, S. Y. *Biomaterials* **2008**, *29*, 4285–4291.
(46) Jackler, G.; Steitz, R.; Czeslik, C. *Langmuir* **2002**, *18*, 6565–6570.
(47) Norde, W.; Giacomelli, C. E. *J. Biotechnol.* **2000**, *79*, 259–268.
(48) Billsten, P.; Wahlgren, M.; Arnebrant, T.; Mcguire, J.; Elwing, H. *J. Colloid Interface Sci.* **1995**, *175*, 77–82.
(49) Ball, V.; Winterhalter, M.; Schwinte, P.; Lavalle, P.; Voegel, J. C.; Schaaf, P. *J. Phys. Chem. B* **2002**, *106*, 2357–2364.
(50) Henzler, K.; Haupt, B.; Lauterbach, K.; Wittemann, A.; Borisov, O.; Ballauff, M. *J. Am. Chem. Soc.* **2010**, *132*, 3159–3163.
(51) Wittemann, A.; Ballauff, M. *Phys. Chem. Chem. Phys.* **2006**, *8*, 5269–5275.
(52) Regnier, F. E. *Science* **1987**, *238*, 319–323.
(53) Asthagiri, D.; Lenhoff, A. M. *Langmuir* **1997**, *13*, 6761–6768.
(54) Schlenoff, J. B.; Rmaile, A. H.; Bucur, C. B. *J. Am. Chem. Soc.* **2008**, *130*, 13589–13597.
(55) Chen, S. F.; Zheng, J.; Li, L. Y.; Jiang, S. Y. *J. Am. Chem. Soc.* **2005**, *127*, 14473–14478.
(56) Pasche, S.; Textor, M.; Meagher, L.; Spencer, N. D.; Griesser, H. J. *Langmuir* **2005**, *21*, 6508–6520.
(57) Pasche, S.; Vörös, J.; Griesser, H. J.; Spencer, N. D.; Textor, M. *J. Phys. Chem. B* **2005**, *109*, 17545–17552.
(58) Giacomelli, C. E.; Norde, W. *J. Colloid Interface Sci.* **2001**, *233*, 234–240.
(59) Zhuravlev, L. T. *Langmuir* **1987**, *3*, 316–318.